Phytoplankton patchiness and their role in the modelled productivity of a large, seasonally stratified lake

Ingrid Hillmer[a,b,*], *Penelope van Reenen*[c], *Jörg Imberger*[c], *Tamar Zohary*[d]

[a] *Centre for Water Research, The University of Western Australia, 35 Stirling Hwy, Crawley 6009, Western Australia, Australia*
[b] *Department of Civil Engineering, University of Chile, Av. Blanco Encalada 2002, Casilla 228 – 3, Santiago, Chile*
[c] *Centre of Water Research, The University of Western Australia, 35 Stirling Hwy, Crawley 6009, Western Australia, Australia*
[d] *Israel Oceanographic and Limnological Research, Ltd., Yigal Alon Kinneret Limnological Laboratory, P.O. Box 447, Migdal 14950, Israel*

A B S T R A C T

Phytoplankton concentration in Lake Kinneret (Israel) has varied up to 10-fold in space and time, with horizontal patches ranging from a couple of kilometres to a basin scale. Previous studies have used a 1D model to reproduce the temporal evolution of physical and biogeochemical variables in this lake. The question that arises then is how appropriate is a 1D approach to represent the dynamic of a spatially heterogeneous system, where there are non-linear dependencies between variables. Field data, a N-P-Z model coupled to both a 1D and a 3D hydrodynamic model, a 1D diffusion-reaction equation and scaling analysis are used to understand the role of spatial variability, expressed as phytoplankton patchiness, in the modelling of primary production. The analysis and results are used to investigate the effect of horizontal variability in the forcing and in the free mechanisms that affect the growth of patterns. The study shows that the use of averaged properties in a 1D approach may produce misleading results in the presence of localised patches, in terms of both concentration and composition of phytoplankton. The reason lies in the fact that the calibration process of ecological parameters in the 1D model appears to be site and process specific. That is, it depends on the pattern's characteristics and the underlying physical processes causing them. And this is a critical point for the success of numerical simulations under spatial variability. In this study, it is also shown that a length scale based on diffusion and growth rate of phytoplankton could be used as a criterion to assess the appropriateness of the 1D assumption.

Keywords:
Phytoplankton patchiness
Scaling analysis
Ecological modelling
Primary productivity
Lake kinneret

1. Introduction

Phytoplankton heterogeneity is a prominent feature of aquatic ecosystems and has been observed ranging in space from centimeters to the basin scale, and in time from seconds to years. Some of the proposed mechanisms for its formation include: accumulation due to flow regimes interacting with the mobility of the species (Franks, 1997; Bee et al., 1998), non-linear interaction between phytoplankton and zooplankton (Steele and Henderson, 1992; Vilar et al., 2003), and external forcing such as change in nutrient and light regimes leading to differential growth. An important aspect of the appearance of patches is that they may reflect the formation of niches for different species as a result of complex spatial variability of

* *Corresponding author at*: Centre for Water Research, The University of Western Australia, 35 Stirling Hwy, Crawley 6009, Western Australia, Australia. Tel.: +61 8 6488 7561; fax: +61 8 6488 3053.
E-mail address: hillmer@cwr.uwa.edu.au (I. Hillmer).

the underlying environment. These niches control the diversity of the system by allowing coexistence of species and by affecting, in turn, the diversity of assemblage of higher trophic levels (Hutchinson, 1961).

The incorporation of spatial heterogeneity may play an important role in the success of an ecological assessment. In monitoring campaigns, the sampling strategy should be designed to capture the scales of any patches (Dutilleul, 1993; Hillmer and Imberger, 2007b) and a few point samples may be misleading. When modelling aquatic ecosystems, allowing for spatial heterogeneity seems to be a key factor in the evolution of a natural system and its response to external forcing. Hillmer and Imberger (2007a) showed that capturing the variability in an open system was essential to assess the effect of a sewage discharge without the interference of boundary advective fluxes. Murray (2001) showed that spatial scales become more important in the response of the ecosystem as the rate of nutrient input increases; and Brentnall et al. (2003) highlighted the role of patches and their scales in increasing productivity.

The relevance of spatial variability in biomass growth has been already recognised; localised high concentration may be more important than the basin average. Even though these connections are well established, the use of complex models to reproduce the behavior of aquatic systems is rare. Such models require more data to run (Brentnall et al., 2003), the calibration and interpretation processes are made difficult by the requirement of intense spatial data sets (Jørgensen, 1994) and run times are normally longer than simpler models.

Spatial heterogeneity is especially important if non-linear processes occur in the system (Murray, 2001). For example, the growth rate of a species predicted from the basin-scale average of all the dependent variables is not necessarily equal to the average of the actual growth rate computed on a point-by-point basis. Biogeochemical rates depend on patch properties and the model calibration process is subject to the temporal variation of patterns in each study site. Thus, the ecological parameters are intimately dependent not only on the relevant physiological processes, but also on the physical processes determining patchiness. This is an important issue when a set of parameters has been chosen to match field data with a one-dimensional model. As a result, this may yield misleading values of ecological parameters, and hence of rates of internal processes. And this, in turn, may lead to misinterpretation of the dynamic of a system.

In this study, Lake Kinneret is used to investigate the role of spatial variability and its impact on numerical predictions. This study is carried out by comparing results from a 1D and a 3D numerical model. An extensive field-sampling program in 1999 and 2000 constitutes the basis to study the length and time scales of patchiness. The numerical results are compared with the field data to check the performance of the models. An analytical model derived from scaling analysis and the solution of a 1D reaction-diffusion equation is used to investigate and to illustrate the characteristic features of the phytoplankton patterns in the field and in the 3D model. The objective of this study is by no means to reproduce accurately the field data. This study rather intends to understand the implications of using a 1D numerical model to predict phytoplankton biomass in the presence of spatial variability.

2. Site description

Lake Kinneret, Israel, has a surface area of 174 km^2, and an average depth of 24 m (Pollingher and Berman, 1975). It is pear-shaped, with the deepest point in the middle and a gentle slope on the western and southern shores (Fig. 1a). The lake is monomictic; temperature stratification begins in April, and persists through spring, summer and autumn, with turnover in January (winter). The Jordan River supplies ca. 60% of the inflowing water and ca. 70% of the nutrient loading. Its flow peaks in late winter and declines to a minimum in summer (June, July and August; Mero, 1978). In addition to this river, there are several small freshwater and thermohaline streams

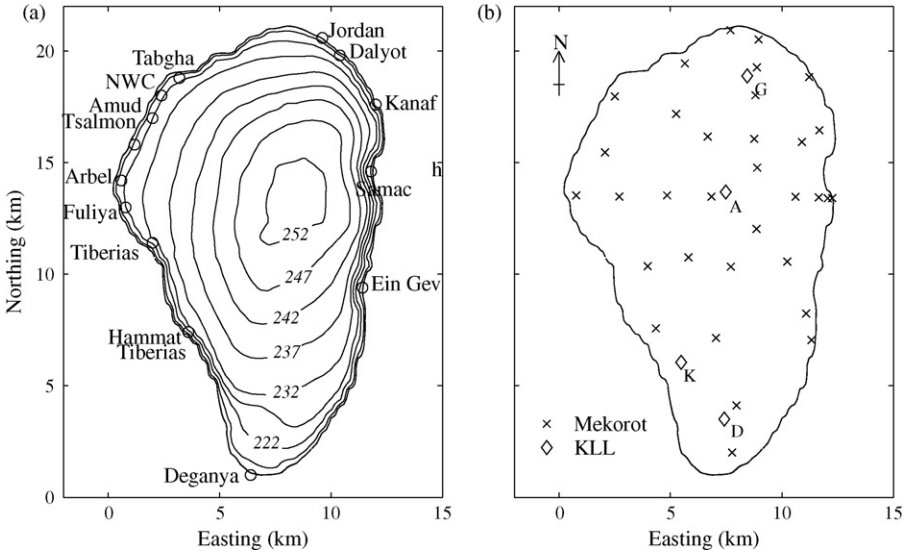

Fig. 1 – Bathymetry of Lake Kinneret (35°30′, 32°40′N) and sampling stations. (a) Contours referenced to mean sea level, and locations of stream inflows and withdrawals (NWC and Deganya) and (b) sampling station locations of the Mekorot Water Company and Kinneret Limnological Laboratory (A, D, G, K).

situated around the shore of the lake (Fig. 1a), which, in addition to runoff, comprise the remaining inflows.

The phytoplankton assemblage and biomass in Lake Kinneret varies seasonally (Berman et al., 1992). The most noticeable is the dinoflagellate *Peridinium gatunense* which forms a typical, intense and high-biomass bloom in spring of most years. Other bloom-forming species have been the diatom *Aulacoseira granulata* (which blooms in winter of some years), the colony-forming coccid cyanobacterium *Microcystis aeruginosa*, and in recent years also nitrogen fixing cyanobacteria such *as Aphanizomenon ovalisporum* and *Cylindrospermopsis cuspis* which bloom in summer-fall (Zohary, 2004a). In addition to those bloom-forming species, the lake hosts a diverse assemblage of non-blooming species, mostly nanoplanktonic species belonging to the Chlorophytes, Cyanobacteria, Diatoms, Cryptophytes and Dinoflagellates. The phytoplankton distribution varies spatially, especially during *Peridinium* blooms; patches of *P. gatunense* ranging from 0.5–2 km in diameter (Berman and Rodhe, 1971) to basin scale (Pollingher and Berman, 1975) have been reported.

The Kinneret zooplankton consists of predatory taxa (adult copepods, predatory rotifers), large herbivores/macrozooplankton (cladocerans, copepodites) and small herbivores or 'microzooplankton' (copepod nauplii, most rotifers, ciliates, heterotrophic flagellates) (Hambright et al., 2007).

3. Methods

3.1. *Field data*

The Kinneret Limnological Laboratory (KLL) of the Israel Oceanographic & Limnological Research has collected water quality data as part of a routine monitoring program. KLL has supplied data for ammonium (NH_4), nitrate (NO_3), total dissolved phosphorus (TDP), soluble reactive phosphorus (SRP), total nitrogen and total phosphorus at weekly intervals on discrete-depth water samples collected from stations A, D and G, and also fortnightly from station K (Fig. 1b). Nutrient concentrations were determined by methods outlined in APHA (1992). Phytoplankton cell counts were conducted fortnightly on Lugol-preserved water samples from 10 discrete depths at station A. The Utermohl (1958) method was used as described by Zohary (2004a). In addition to the above monitoring data from KLL, the Mekorot Water Company supplied nutrient (NH_4, NO_3, TDP, SRP, total nitrogen, total phosphorus) and chlorophyll data from Lake Kinneret collected monthly at 33 stations until April 2000 and fortnightly at 16 stations afterwards (Fig. 1b).

3.2. *Numerical models*

The Computational Aquatic Ecosystem Dynamics Model (CAEDYM) is coupled with the 3D hydrodynamic model, Estuary and Lake Computer Model (ELCOM), and with the 1D hydrodynamic model, Dynamic Reservoir Simulation Model (DYRESM). In this way, the coupled models simulate the hydrodynamic, nutrient cycles and food web dynamics in the lake in 3D and 1D.

3.2.1. *1D hydrodynamic model*

DYRESM is a pseudo 1D Lagrangian layer model that simulates vertical variations, where 3D processes are accounted for with parametric descriptions (Yeates and Imberger, 2004). The horizontal layers have uniform properties and their thickness vary between user-defined limits (Imberger and Patterson, 1990). The surface layer mixing is the result of wind stirring, convective overturn and wind shear, while internal mixing depends on the value of the Lake Number (Imberger and Patterson, 1990). The inflows are modelled by adding the input to the appropriate layer, with the specified temperature, salinity and water quality.

3.2.2. *3D hydrodynamic model*

The 3D model, ELCOM, solves the hydrostatic, Boussinesq, Reynolds-averaged Navier Stokes and scalar transport equations with an eddy-viscosity approximation for horizontal turbulence (Hodges et al., 2000). ELCOM uses a conservative ULTIMATE QUICKEST scheme for scalar transport, an Euler-Lagrange scheme for advection of momentum, and a semi-implicit method for free surface evolution (Laval et al., 2003). Following Laval et al. (2003), a filter is applied to correct for vertical mixing due to numerical diffusion. In this case, the filter is calibrated using field data. For these simulations, ELCOM-CAEDYM is run on a grid of 400 m × 400 m × 1 m and a time step of 5 min.

In Lake Kinneret, horizontal transport in the surface layer has been found to be dominated by internal wave motions over scales of days. For longer periods, horizontal shear dispersion due to wind forcing was the dominant mechanism (Stocker and Imberger, 2003). The combination of these processes yielded a horizontal dispersion coefficient of 17.1 $m^2\,s^{-1}$ over the stratified period (Stocker and Imberger, 2003). This value is applied in ELCOM from April to December when the water column is stratifying and stratified. When the water column is mixed (January to March), the mechanism that contributes to enhance the dispersion coefficient no longer exists and a reduced value is expected. For this period, the dispersion coefficient is set to 0.2 $m^2\,s^{-1}$ for a grid cell of 400 m (Okubo, 1971).

3.2.3. *Ecological model*

The ecological model is based on the 'N-P-Z' (nutrient-phytoplankton-zooplankton) type, but it also includes comprehensive descriptions of carbon, nitrogen, phosphorus, oxygen and silica. CAEDYM is a complex model and only a brief description is given here; more information can be found in Bruce et al. (2006).

The model includes a range of biological state variables including 5 phytoplankton, 3 zooplankton and 1 group of heterotrophic bacteria. The five groups of phytoplankton modelled in this study are 'Peridinium' (the dinoflagellate *P. gatunense*), 'Microcystis' (*M. aeruginosa*), 'N_2-fixing cyanobacteria' (*A. ovalisporum* and *C. cuspis*), 'nanophytoplankton', and 'diatoms' (*Aulacoseira granulate*). The phytoplankton dynamics is characterised by growth, mortality, excretion, respiration, grazing, settling and resuspension. Growth is limited by nitrogen, phosphorus and light (and silica in the case of diatoms). The model uses a dynamic intracellular store for nitrogen and phosphorus that regulates the growth rate. Phytoplankton is

modelled as carbon converted into chlorophyll using constant C:Chla ratios (=67, 150, 27, 45 and 32 mg C (mg Chla)$^{-1}$ for Peridinium, Microcystis, N_2-fixing cyanobacteria, nanoplankton and diatoms, respectively). The vertical migration and settling is defined differently for each group. Peridinium and Microcystis have the capacity to move vertically along the water column. Their vertical migration is regulated by the need for light and nitrogen (Kromkamp and Walsby, 1990). N_2-fixing cyanobacteria and nanoplankton follow Stoke's law that allows for changes in intracellular density. The diatoms group is assigned a constant settling velocity.

Three groups of zooplankton, defined by their ecological role, are configured. They are the predators, large herbivores, and microzooplankton. Each zooplankton group is characterised by a feeding (predation or grazing), mortality, respiration, egestion (fecal pellets) and excretion component. Each group is assigned a feeding preference for each of the 5 phytoplankton groups, the other zooplankton groups, detrital material and bacteria. The predators feed on all of the other zooplankton groups while the large herbivores graze mainly the nanoplankton. The microzooplankton consumes particulate organic carbon and bacteria.

The organic and inorganic forms of carbon, nitrogen, phosphorus and silica cycles are modelled as both filterable and particulate pools. In general terms, the processes affecting nutrients are: dissolved sediment fluxes, particle resuspension, particle settling, organic particle decomposition, dissolved organic mineralisation, adsorption/desorption of dissolved inorganic nutrient to inorganic particles, mortality and excretion from aquatic flora and fauna, autotrophic uptake of dissolved inorganic nutrients and respiration by algae, zooplankton and bacteria. Atmospheric gas exchange between dissolved carbon dioxide and the atmosphere is also explicitly modelled.

The parameters for the ecological model were obtained both from experimental analysis on phytoplankton (Zohary, 2004b) and zooplankton (Hambright et al., 2007) in Lake Kinneret, and from the literature. The following parameters were measured experimentally for some or all of the 5 phytoplankton groups simulated: phosphorus uptake kinetics parameters (turnover time, maximum uptake rate, bioavailable P), growth rate as a function of water temperature and related parameters (optimum temperature, maximum temperature, Q_{10}), cellular quotas of C, N, P, Chl *a*, dry weight and wet weight. In situ nitrification rates were measured using ^{15}N. Measurements of bacterial abundance, size and biomass, production and respiration rates were also conducted. The ecological parameters used in this study were set after a sensitivity analysis of the parameters was carried out using the 1D model simulations over a 2-year period (1997–1998; M. Hypsey, personal communication, 2006; Zohary et al., 2006).

3.2.4. *Models set-up*

The simulations are carried out for a period of 160 days, starting in November 1999; from the end of the stratified period to the onset of the stratification period in spring. The same inflow and meteorological data and initial conditions for all the variables needed are used in both models (1D and 3D). The simulations are carried out with only one inflow, the Jordan River. The Mekorot data are used for the initial conditions, after averaging them over the sampling stations. Temperature data collected at station A is used to initialize the model runs. Meteorological data from Tabha, 1 km offshore from KLL, is used to force the free surface. The same ecological parameters are also applied in the simulations with the 1D and 3D hydrodynamic model.

3.3. *Patches: analytical model*

Patchiness of phytoplankton can occur with different patterns and length scales depending on the underlying physical mechanisms that affect their evolution. For instance, bands of dense concentration of organisms are characteristic of internal wave, while sharp transitions may be generated by fronts (Chiffings and McComb, 1981; Franks, 1997). Several studies, using constant growth rate (KiSS model; Kierstead and Slobodkin, 1953; Hillmer and Imberger, 2007a) and non-linear dynamic population (Steele and Henderson, 1992; Brentnall et al., 2003), have shown the role of diffusion and biological processes in determining the length scale of the patterns, as their relative importance varies.

In order to investigate the underlying mechanisms responsible for patchiness in Lake Kinneret and to assess the role of the biogeochemical and dispersive processes, the analytical solution of the 1D diffusion-reaction equation is used. The 1D equation is:

$$\frac{\partial C}{\partial t} = \frac{\partial}{\partial x}\left(k\frac{\partial C}{\partial x}\right) + \mu(x,t)C \tag{1}$$

where x is the spatial coordinate, t the time, C the phytoplankton concentration, k is the diffusion coefficient (e.g. m^2 s^{-1}) and μ is the net growth rate (e.g. s^{-1}). The analytical solution of this equation, in a still water column, after applying scaling analysis, and with the initial condition defined by a Dirac delta function, is given by (Hillmer and Imberger, 2007a):

$$C^*(\xi,\tau) = \frac{M^*}{\sqrt{4\pi\tau}}\exp\left(-\frac{(\xi)^2}{4\tau}\right)\exp(\tau) \tag{2}$$

where $\xi = x/L$, $\tau = t/T$ and $C^* = C/C_0$ are the scaled variables and C_0 (μg Chla L^{-1}) is the maximum concentration. The characteristic length and time scales have been chosen as $L = (k/\mu)^{1/2}$ and $T = 1/\mu$ respectively. The slug of mass, $M^* = M/C_0$, is introduced initially at the origin. This solution shows the evolution of a phytoplankton patch subject to the interaction between diffusion and growth rate.

In this study, the boundary of a patch of phytoplankton is defined arbitrarily as the distance at which the concentration is 30% of the maximum concentration in the patch. An effective radius of the patch is calculated as the square root of the area of a closed contour associated with the boundary concentration (30% of the maximum). The concentration gradient within the patch is then obtained by estimating an effective radius for different specific concentrations in the patch, after subtracting the background concentration.

The analytical solution obtained (Eq. (2)) is then compared with the phytoplankton concentration of horizontal patches observed in the field and in the 3D simulation. This is done by applying a least-squares fit of the analytical solution to the

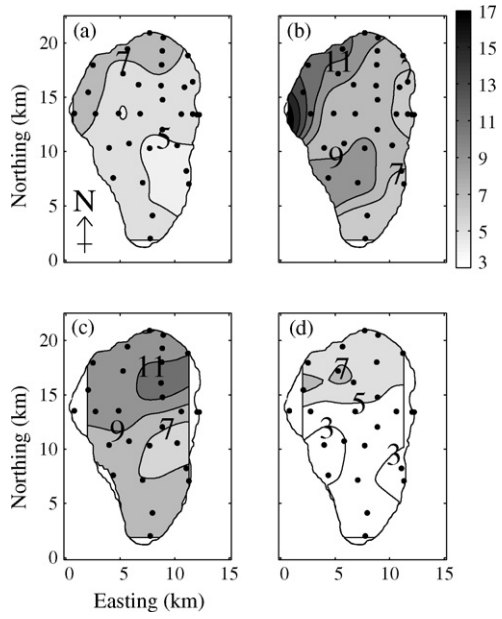

Fig. 2 – Spatial distribution of chlorophyll concentration averaged over the upper 10 m of the water column. (a) 31 October 1999, (b) 1 February 2000, (c) 1 May 2000 and (d) 18 July 2000. Data were collected from the field-sampling stations marked by dots.

concentration gradient of the patches. This analytical solution is evaluated at $\tau = 1$, the time equal to the growth time scale, $1/\mu$. A value of 17 $m^2\ s^{-1}$ for the dispersion coefficient is used for data between April and December. For the rest of the time, the coefficient is estimated as a function of the scales of the patches (Okubo, 1971). A patch-averaged net growth rate is obtained in the field and in the model as a result of the least-squares fitting process.

4. Results and discussion

4.1. *Spatial patterns*

Several mechanisms may explain the origin of phytoplankton patches in Lake Kinneret (Fig. 2). For instance, field observations showed that during winter the Jordan River inflow is diverted westwards after entering the lake and continues southwards along the western shore of the lake. This behavior of the flow is due to the action of the Coriolis forcing that generates a counterclockwise circulation in the lake (Serruya, 1974). 3D simulations with a conservative tracer corroborated this behavior (not shown). Thus, the Jordan River acting as a source of nutrients enhances the productivity along the western side during the late winter months. Another factor that may favor heterogeneous conditions is light. Light is a limiting factor for growth when the depth of the mixed surface layer is larger than the trophogenic depth. In this case, the phytoplankton assemblage does not have sufficient light for growth as they are mixed down in the water column (Huisman et al., 1999; Ptacnik et al., 2003). In this lake, light appeared more available near the western shore of the lake where the surface layer was consistently shallower due to the westerly winds. Motile species are also likely to cause patchy conditions, since their movement capabilities make them less susceptible to vertical shear and thus feel a smaller rate of horizontal dispersion. In summary, the effect of the Jordan River, the spatially variable light limitation and the presence of motile species represent sources of spatial variability of phytoplankton in this lake.

Field data and 3D numerical results, averaged over the upper 10 m of the water column, are analysed to determine the characteristic length scale of the patterns and to identify the main processes involved in their evolution. The results of the least-squares fit using Eq. (2) show that the concentration curves of the patches, obtained from the analytical solution, field data and numerical data, coincide. This indicates that the evolution of the patches studied is similar and governed by the same processes. Thus, from this analysis, the horizontal dispersion coefficient and the rate of phytoplankton growth appear to control the size of the patches, whereas, as mentioned above, different mechanisms may influence the degree of patchiness and the geographic location within the lake.

In the field, the size of the patches varies approx. between 4.5 and 9 km without any seasonal trend (Table 1). This lack of seasonal variation is attributed to the correspondence between low values of growth rate and diffusion coefficient, during the non-stratified period, and high values of growth rate and diffusion coefficient, during the stratified period (Berman and Pollingher, 1974; Serruya, 1975). The 3D simulation shows patches varying from 1.5 to 7 km, with smaller patches during the non-stratified period. This analysis yielded an almost constant growth rate during the simulation period (Table 1). Overall, the results show that the 3D model is able to capture the scale of the patterns by properly reproducing the role of horizontal diffusion and biogeochemical processes in their formation.

The results show that the size of the patches, L_p, from both the field and the 3D model are one to three times $L = (k/\mu)^{1/2}$, the length scale at which diffusion balances the growth rate (Table 1). Thus, it could be stated that patches from the field and the simulations have a very similar characteristic length scale, proportional to the square root of the diffusivity ($\sim k^{1/2}$; Table 1; Fig. 3). This parameter can be used to estimate the response of a system to a perturbation by distinguishing different kind of patterns' evolution. For instance, when $k/\mu \rightarrow$ (basin scale)^2, a patch generated by an external forcing would be eventually limited by the basin scale. In contrast, when $k/\mu \ll$ (basin scale)^2, a patch would tend to grow locally in a confined area. Hence, L can be used as a criterion to validate the assumption of the one dimensionality of phytoplankton patchiness: if L is much larger than the basin scale, the system is expected to be characterised by a homogeneous horizontal concentration. In the case of Lake Kinneret, the 1D assumption, valid when $k/\mu \gg$ (basin scale)^2, does not appear to be appropriate. However, the potential impact of applying this assumption on modelled evolution of the phytoplankton biomass is assessed in the next sections. The comparison between a 1D and a 3D model is used to address the issue of differences in the patterns' behavior imposed by the relationship between horizontal diffusion and phytoplankton growth.

Table 1 – Characteristic of patches in the field and in the 3D model

Sampling time	k ($m^2\ s^{-1}$)	L_p (km)	μ (d^{-1})	T (d)	r^2	L (km)
Field data						
31/10/1999	17	8.6	0.11	9.1	0.98	3.7
31/10/1999	17	4.4	0.43	2.3	0.99	1.8
28/11/1999	17	7.7	0.41	2.4	0.98	1.9
2/1/2000	17	9.3	0.06	16.7	0.98	4.9
1/2/2000	6.3	7.9	0.07	13.9	0.97	2.7
28/2/2000	6.8	7.8	0.05	20.4	0.97	3.5
4/4/2000	17	4.6	0.40	2.5	1	1.9
1/5/2000	17	7.9	0.12	8.3	0.99	3.5
3D model						
12/12/1999	17	7.2	0.15	6.7	1	3.1
31/12/1999	17	7.1	0.12	8.3	0.998	3.5
16/1/2000	2.3	3.4	0.22	4.5	0.92	1.0
8/2/2000	0.9	1.5	0.23	4.3	0.98	0.6
19/3/1999	1.7	2.6	0.19	5.3	0.97	0.9
22/3/1999	17	2.7	1.40	2.9	0.99	1.0
31/3/1999	17	6.0	0.19	5.3	0.98	2.8

k represents the diffusion coefficient, L_p represents the size of the patch, μ is the growth rate, T is the growth time scale ($1/\mu$), r^2 is the correlation coefficient (obtained from the least-squares fit of the analytical solution to the concentration gradient of the patches observed in the field and in the 3D numerical results), and L is the characteristic length scale.

4.2. *Comparison of results between the 1D and 3D numerical models*

4.2.1. *Chlorophyll concentration*

Phytoplankton biomass in Lake Kinneret is generally dominated by the dinoflagellate *P. gatunense* in spring (Berman and Pollingher, 1974). But from November 1999 to October 2000, the phytoplankton biomass appears to consist mainly of nanoplankton, with Peridinium as the second group, according to KLL data (not shown). The numerical results from both models, volume-averaged over the upper 10 m of the water column, maintain overall the dominance of nanoplankton and Peridinium over the other phytoplankton groups (Fig. 4). However, the results show some difference between the two models, especially after Feb. In this second half of the simulation period, the biomass of nanoplankton and Peridinium grows higher in the 1D than in the 3D model, and by March the dinoflagellate clearly dominates in the 1D simulation.

In the 1D model, the total chlorophyll (Chl *a*), averaged over the 10 m surface layer, remains constant with time (after the

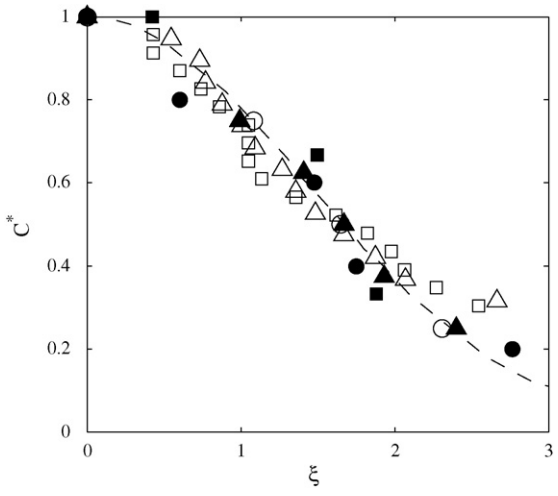

Fig. 3 – Comparison of patch characteristics from field data and 3D simulation using a 1D diffusion-reaction equation on: 31 Oct 1999 (●, field data), 12 Dec 1999, (○, model results), 1 Feb 2000 (■, field data), 8 Feb 2000 (□, model results), 4 April 2000 (▲, field data) and day 22 March 2000 (△, model results).

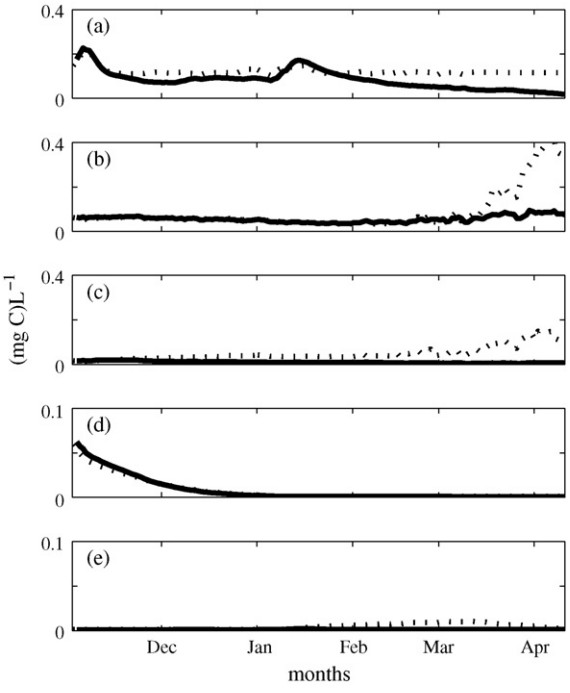

Fig. 4 – Comparison of phytoplankton biomass between simulations with 1D (dotted line) and the 3D (thick line) models. (a) nanophytoplankton, (b) Peridinium, (c) Microcystis, (d) N_2-fixing cyanobacteria and (e) diatom.

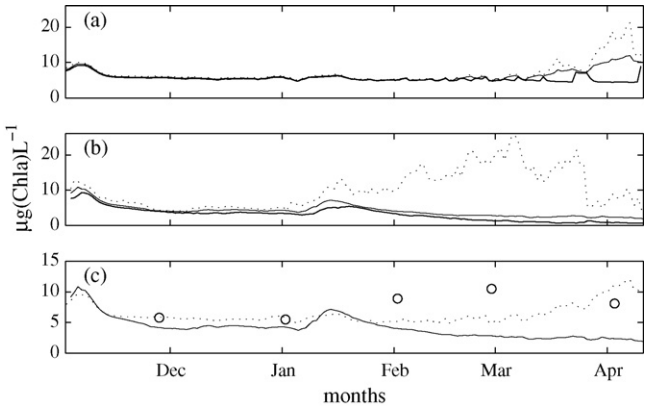

Fig. 5 – Temporal evolution of total chlorophyll over the 10-m surface layer expresses as: (a) volume-averaged (thick line), minimum (thin line) and maximum (dotted line) calculated for the 3D model, (b) volume-averaged (thick line), minimum (thin line) and maximum (dotted line) calculated for the 1D model and (c) comparison between the volume-averaged 1D model (dotted line), volume-averaged 3D model (thick line) and field data (○).

spin-up of the model) until March (Fig. 5a). Afterwards, the Chl *a* begins to increase due to the increase in the biomass of Peridinium and Microcystis (see Fig. 4b and c). These species produce a vertical gradient as it can be concluded from the difference between maximum, mean and minimum Chl *a* in the upper 10 m of the water column. In the 3D simulation, two periods can be observed (Fig. 5b). During Nov and Dec, the average concentration of Chl *a* remains stable (after the *spin-up* of the model) with a low variability expressed as $Chla_{max}/Chla_{min} < 3$, where $Chla_{max}$ and $Chla_{min}$ are the maximum and minimum Chl *a* concentration in the upper 10 m of the surface layer. During the second period (Jan to April), Chl *a* has a peak concentration in January that coincides with the increase in the nutrient input from the Jordan River. Then, the mean concentration decreases again to reach a new lower stable value, while the variability, $Chla_{max}/Chla_{min}$, increases to 28. Unlike the 1D simulation, the increase of the *Peridinium* and *Microcystis* when the stratified period begins is not observed.

From Fig. 5c, it is possible to observe that the predicted mean chlorophyll concentration is similar for both models, and also compare well with field data (monthly averaged over the 10 m surface layer) for the first two months. For the remaining months, however, these three data sets clearly diverge.

4.2.2. *Factors affecting the difference in chlorophyll in the models*

To gain insight into the reasons for the difference in Chl *a* between the two models, other physical, biological and chemical variables are analysed. In terms of the hydrodynamics, since the 1D model only simulates vertical variations, the only possible comparison between the two models is by investigating the temperature vertical structure. In addition, the nutrient concentration in the water column and the physiological condition of the phytoplankton is investigated. These variables are volume-averaged over the 10 m surface layer.

4.2.2.1. Vertical temperature structure. Comparison between the vertical temperature profile of the 1D simulation and of the station A in the 3D simulation (see Fig. 1 for location) shows that both models present a similar temporal evolution, with some differences during March and April, when the thermocline deepens and the surface temperature increases (Fig. 6b and c). Although these differences could lead to different turbulent conditions, and hence, affect the development of *Peridinium* (Pollingher and Zernel, 1981; Thomas and Gibson, 1990), this factor does not seem to provide a satisfactory explanation for the divergence in the Chl *a* concentration. In addition, both models' result agree well with field data from station A (Fig. 6).

4.2.2.2. Nutrient concentration in the water column. The simulated concentration of ammonium (NH_4) and nitrate (NO_3) from both models and field data, all averaged over the 10 m surface layer, follow a similar trend (Fig. 7). In contrast, the concentration of phosphorus (PO_4), averaged over the 10 m surface layer, is larger in the 1D than in the 3D simulation during Nov and Dec, although they become similar during the Jordan River inflow period (Fig. 8). Both numerical results yield values of phosphorus (PO_4) between 1 and 2 orders of magnitude smaller than the observed in the field

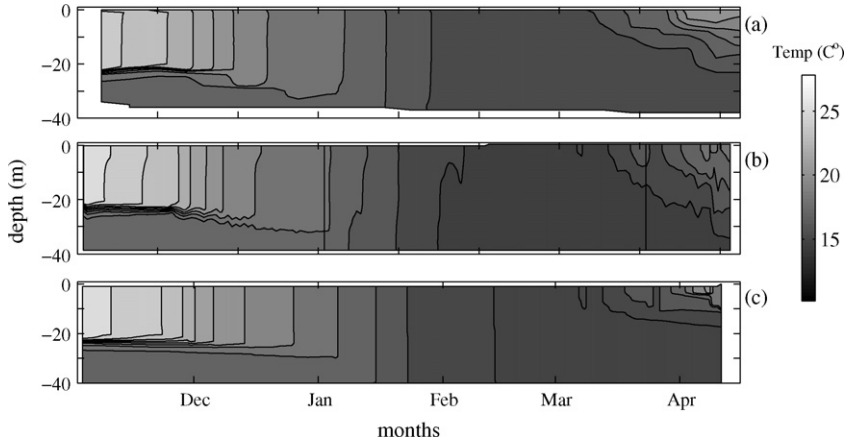

Fig. 6 – Vertical temperature structure at station A. Comparison between (a) field data, (b) 3D simulation and (c) 1D simulation.

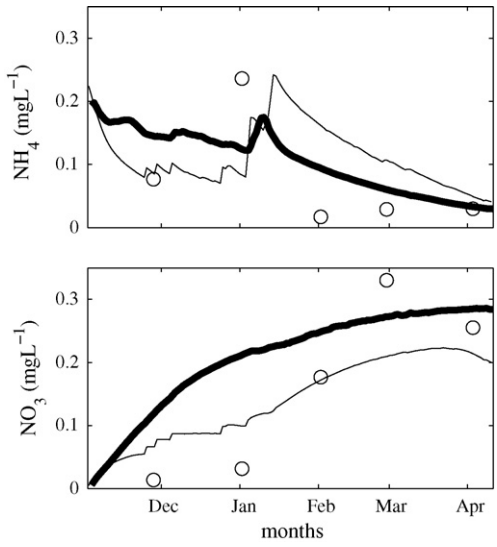

Fig. 7 – Comparison between numerical results from the 1D (thin line) and the 3D (thick line) simulations for ammonium (NH_4) and nitrate (NO_3) averaged over the upper 10 m of the water column. The symbol ○ represents field data averaged monthly of the spatial sampling.

data. Discrepancies on the phosphorus data between field and numerical results have also been obtained in previous studies. Bruce et al. (2006), using a different configuration for the coupled DYRESM-CAEDYM (1D model), also obtained a poorer match in the phosphorus data than in the rest of the variables when replicating the field data. In this regard, the quality of the phosphorus analysis by Mekorot at low concentrations in the surface waters has been questioned. Hence, for the purpose of this study the results obtained here are considered acceptable. In any case, the low concentration of PO_4 suggests that it is cycled rapidly through the biota in the water column.

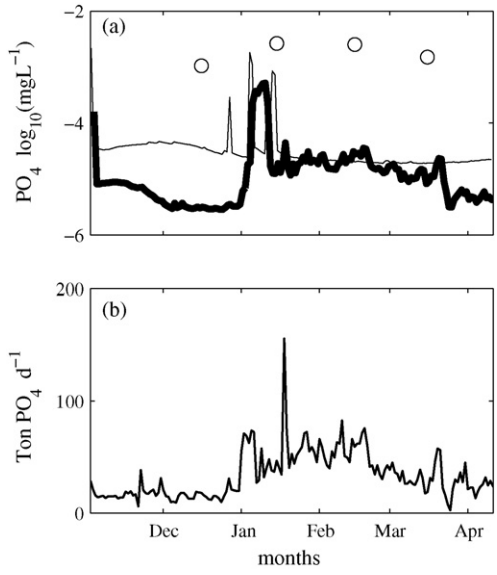

Fig. 8 – Temporal evolution of the phosphate concentration in the lake and phosphate from the input. (a) Comparison between numerical results from the 1D (thin line) and the 3D model (thick line) for phosphate (PO_4) averaged over the 10 m surface layer. The symbol ○ represents field data averaged monthly over the spatial sampling arrangement. (b) Input of (PO_4) from the Jordan River.

4.2.2.3. *Phytoplankton physiological condition*. The physiological condition of the phytoplankton is studied by analysing the phosphorus limitation function used in the ecological model, averaged over the upper 10 m of the water column. Phosphorus is chosen since this is the main limiting nutrient for the main phytoplankton group (nanoplankton and Peridinium). The limitation function is given by:

$$f(P) = \left(\frac{\mathrm{IP}_{\max}}{\mathrm{IP}_{\max} - \mathrm{IP}_{\min}}\right)\left(\frac{\mathrm{IP} - \mathrm{IP}_{\min}}{\mathrm{IP}}\right) \quad (3)$$

where IP is the internal phosphorus concentration, and $\mathrm{IP}_{\max}$ and $\mathrm{IP}_{\min}$ are the higher and lower parameters for the internal phosphorus concentration set in the ecological model. This limitation function varies from 0 to 1, and the higher its value the less limited the phytoplankton is due to phosphorus. During Nov and Dec, both the mean and the maximum value for the limitation function in the 3D model are equal or lower than the mean value obtained from the 1D model (Fig. 9). This situation is reflected in the total chlorophyll; mean and maximum values from the 3D model are equal or lower than the 1D results. The lower phosphorus availability in the 3D model seems to be accounted for by the lower phosphorus concentration during this period (Fig. 8).

During the remaining months (Jan–Apr), the situation is clearly different. Phosphorus from the Jordan River is incorporated in the system producing an abrupt increase in the averaged limitation function in both models (Fig. 9). The implications of this increase are only apparent in the chlorophyll concentration of the 3D simulation (Fig. 5). In this case, the Chl *a* increases is due to the response of the nanoplankton, since the biomass of Peridinium is not affected. After this peak, the mean limitation function decreases in both phytoplankton groups, and in both models. However, a high maximum limitation function remains in the 3D simulation. The results also shows that both group of phytoplankton present different physiological conditions, with nanoplankton the most phosphorus limited in both models, and thus the more susceptible to changes in phosphorus availability. A comparison between conservative tracer and phosphorus behavior obtained from the 3D simulation (not shown) shows that the nutrients entering the system are taken up very fast, before being dispersed, which make them unavailable to the rest of the lake. This results in a localised effect that is especially evident in the nanoplankton behavior. Thus, the input from the river leads to an increase in the limitation function (or a decrease in phosphorus limitation) that explains the behavior of the maximum and mean limitation function described previously.

4.2.3. *Patterns in the system*

To understand the dynamic of the formation of patches, their characteristics are analysed in terms of the physiology of the phytoplankton constituting them. The spatial correlation coefficient between the chlorophyll concentration and the phosphorus limitation function, obtained from the 3D simulations, is calculated to assess their relationship (Fig. 10). Both

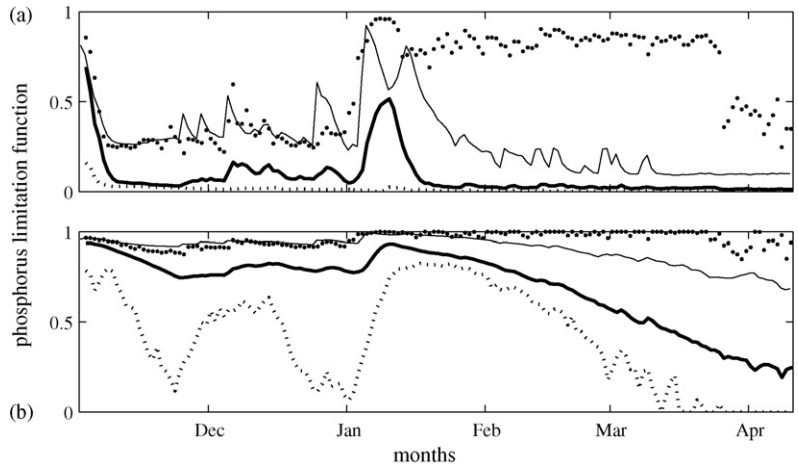

Fig. 9 – Phosphorus limitation function in the 10-m surface layer. Volume-averaged (thick line), minimum (dotted line) and maximum (♦) calculated from the 3D numerical results and volume-averaged calculated from the 1D numerical results (thin line) for (a) nanoplankton and (b) Peridinium.

biomass and limitation function are volume-averaged over the upper 10 m of the water column. In particular, nanoplankton and Peridinium biomass, as the main phytoplankton groups, and their phosphorus limitation functions are analysed. In the case of nanoplankton, the results show that, except from Dec to middle Jan (after the *spin-up* period) when the correlation reaches very low values, patches with higher chlorophyll concentration are associated with higher limitation function, or equivalently, lower internal phosphorus limitation. The low correlation, during Dec and Jan, indicates that nutrients are not an important factor and patches arise by other mechanisms, whereas the increase in nutrients due to the Jordan River seems to have generated the increase in Chl *a*. As for *Peridinium*, the situation is completely different (Fig. 10); there is a low and negative correlation between internal availability of phosphorus and *Peridinium* biomass during most of the simulation period. This implies, again, that there are other factors, rather than phosphorus, triggering the generation of patches (for instance, their motility), even though the increase in the phosphorus input from the river affected the Peridinium evolution, to some extent, as the evolution of the limitation function suggested.

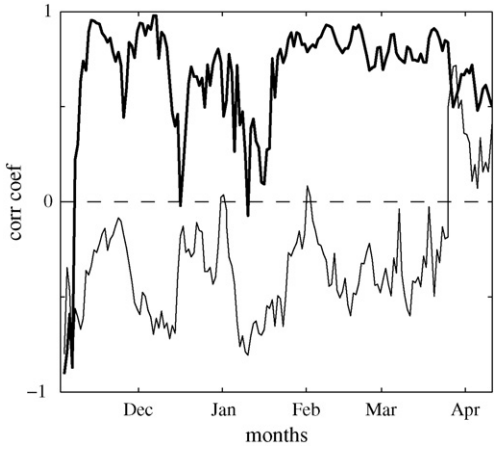

Fig. 10 – Temporal evolution of the correlation coefficient between phytoplankton biomass and its limitation function calculated from the 3D simulation. Nanoplankton is represented by a thick line and Peridinium by a thin line.

In summary, the Chl *a* from the two models shows overall similar trends, although there are some differences, especially in the second half of the simulation period. During the first period (Nov–Jan), the effect of the internal cycling is more important than the effect of the external input. Also, there are no major patches in terms of concentration or variability. Therefore, the observed differences could be attributed mainly to intrinsic differences, that is, to differences in the internal processes in the models due to spatial variations in the lake given by the set-up. These differences, however, could be considered low in practical terms, and also considering the uncertainties associated with some ecological parameters in the model. In the second period, the nutrient input becomes more important. The input from the Jordan River proves to be a source of patchiness, increasing the degree of heterogeneities in terms of variability, that added to the intrinsic differences observed between the two models in the first period, results in a higher divergence between the 1D and the 3D results. In this study, we focus on the second source of differences expressed as phytoplankton patchiness.

4.3. *Effect of different mechanisms of constraints in phytoplankton biomass distribution: 1D vs. 3D*

The occurrence of patches requires two conditions: a forcing mechanism and a free mechanism for the growth of patterns. The forcing mechanism refers to an external forcing or perturbation that generates the differential concentration. The free mechanism controls the evolution of the patches; for instance, dispersion. The dispersive processes, acting against the formation of patterns, are balanced by the phytoplankton growth to maintain the patches. The 3D and 1D approaches differ radically in the way that forcing and free mechanisms are modelled horizontally. In the 1D approach, forcing is represented as if it was spatially uniform. In the case of

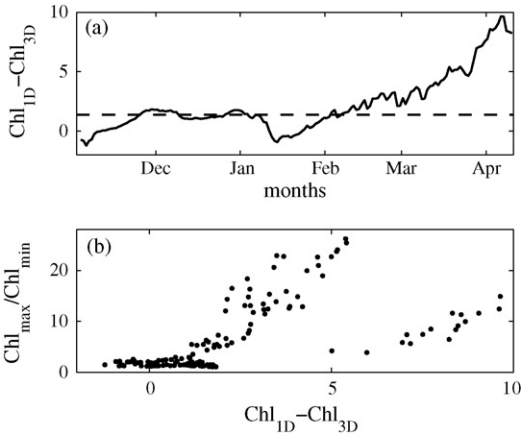

Fig. 11 – Effect of patches in modelled phytoplankton concentrations. (a) Temporal evolution of the difference in total chlorophyll between the 1D and the 3D model in the 10-m surface layer and (b) intensity of variability (Chl_{max}/Chl_{max}) in the 3D model results in the 10-m surface layer as a function of the difference in total chlorophyll between the 1D and the 3D model in the 10 m surface layer. The symbol (–) represents the mean of the background difference.

diffusion, it is represented as if it acted rapidly enough to stop patches from forming. The implications of this lack of horizontal heterogeneity in the 1D approach for phytoplankton biomass are investigated by analysing the extent of variability in the system as a function of the difference between the Chl *a* from the 1D and 3D simulations (Fig. 11a). Low differences between the two models (<2 μg (Chla) L^{-1}) correspond to low variability ($Chla_{max}/Chl_{min} < 5$). Differences between the two models from 2 to 6 μg (Chla) L^{-1} correspond to a variability between 5 and 28. And high differences between the two models (6–10 μg (Chla) $L^{-1)}$ are associated with medium variability varying from 5 to 15.

The difference, as explained before, during the low variability period is attributed to intrinsic differences between the models, and yields a value of 1.5 μg (Chla) L^{-1}. This value is calculated during Dec when the concentrations showed a stable behavior. It is assumed that this value represents the background or intrinsic difference during the rest of the simulation (Fig. 11b). During the period with high variability, i.e. from Jan to March, when the difference may be associated only with the heterogeneity caused by the nutrient input, the mean difference in concentration of chlorophyll between the 1D and the 3D model is 2.5 μg (Chla) L^{-1} (above the intrinsic difference calculated). This represents a reduction in concentration of almost 30% over the 1D results. During the last period, a mean difference in concentration of 5 μg (Chla) L^{-1} is observed, representing a 40% reduction over the 1D results. In this case, though, the difference originates from the capability of the motile species (*Peridinium*) to migrate and grow in the 1D model, by taking advantage of the changes in the temperature and stratification. The 3D model could not reproduce this situation as the nutrient-limited physiological condition is much higher and thus the phytoplankton is unable to recover even under favorable physical conditions.

5. Conclusions

It is shown that the horizontal diffusion plays a key role in the evolution of patches in Lake Kinneret. The input from the Jordan River is a strong source of patchiness, while the motility of phytoplankton is shown to combat horizontal shear dispersion and thus leads to smaller size patches.

Differences in the representation of forcing and free mechanisms of patterns' growth may lead to different results when modelling phytoplankton abundance and temporal dynamics. Results from the 3D and the 1D approach applied in Lake Kinneret present differences (30%) in the basin scale averaged chlorophyll concentration, using the same ecological model parameters. Results suggest that the variability due to the formation of marked patches plays a role in these differences. Although these differences may not be considered dramatic for the simulation period of this study, they highlight the fact that the 1D and 3D models diverge. This divergence, as it was shown, becomes evident during the period when patches presented more variability due to a very localised input source. In addition, an important point that needs to be considered is that this divergence could increase as the simulation is extended. And this could lead to totally different scenarios, not only with different Chl *a* concentration but also different phytoplankton composition, as it is observed during the last month of the simulation.

As mentioned before, the question that arises is how appropriate is a 1D model to study the dynamic of a heterogeneous system. This question is especially relevant in the presence of phytoplankton patches in the system, where differential physiological and biogeochemical characteristics interact with non-linear processes. Under these conditions, the biomass average is not necessarily linearly related to the averaged environment. The results in this study indicate that, even though a 1D model may satisfactorily reproduce the vertical temperature characteristic in a lake, this is no guarantee that such a model is satisfactory for simulating the ecological behavior. Satisfactory results may not be achieved, unless the ecological parameters are calibrated for each condition imposed by physical processes. In other words, the choice of ecological parameters appears to depend on the pattern's dynamics, e.g. not only on the formation, evolution and properties of the patterns but also on the variation of the underlying physical processes causing them. This implies that the calibration process in a 1D approach is both site and processes specific; it implicitly incorporates the effect of the presence of patchiness, caused by physical factors, into the physiological description of the state variables in the 1D ecological model. Clearly, such a procedure is good for interpolating lake behavior, but will produce poor results when used to extrapolate the ecological response of a lake to a new type of forcing.

Finally, in this study the length scale given by $(k/\mu)^{1/2}$ appeared as a criterion to estimate the capability of the system to generate patches and assess the appropriate approach. However, the differential concentration that may result from the patches generation required a 3D model simulation to assess the quantitative impact on the total biomass.

Acknowledgments

The authors thank the Yigal Alon Kinneret Limnological Laboratory and Mekorot Water Company for providing the data used in this study. We give thanks to Matthew Hipsey for his valuable help with the set-up of the ecological model and DYRESM, and Matthew Rafty for his help regarding DYRESM. We also thank Jose Romero for his helpful comments on the manuscript.

REFERENCES

Bee, M.A., Mezic, I., McGlade, J., 1998. Planktonic interactions and chaotic advection in Langmuir circulation. Math. Comput. Simul. 44, 527–544.

Berman, T., Pollingher, U., 1974. Annual and seasonal variations of phytoplankton, chlorophyll and photosynthesis in Lake Kinneret. Limnol. Oceanogr. 19, 31–54.

Berman, T., Rodhe, W., 1971. Distribution and migration of *Peridinium* in Lake Kinneret. Mitt Int. Verein. Limnol. 19, 266–276.

Berman, T., Yacobi, Y., Pollingher, U., 1992. Lake Kinneret phytoplankton: stability and variability during twenty years (1970–1989). Aquat. Sci. 54, 104–126.

Brentnall, S., Richards, K.J., Brindley, J., Murphy, E., 2003. Plankton patchiness and its effect on larger-scale productivity. J. Plankton Res. 25, 121–140.

Bruce, L.C., Hamilton, D.P., Imberger, J., Gal, G., Gophen, M., Zohary, T., Hambright, K.D., 2006. A numerical simulation of the role of zooplankton in C, N and P cycling in Lake Kinneret, Israel. Ecol. Modell. 193 (3–4), 412–436.

Chiffings, A.W., McComb, J., 1981. Boundaries in phytoplankton populations. Proc. Ecol. Aust. 11, 27–38.

Dutilleul, P., 1993. Spatial heterogeneity and the design of ecological field experiment. Ecology 74 (6), 1646–1658.

Franks, P.J.S., 1997. Spatial patterns in dense algal blooms. Limnol. Oceanogr. 42 (5), 1297–1305.

Hambright, K.D., Zohary, T., Güde, H., 2007. Microzooplanktondominate carbon flow and nutrient cycling in a warm subtropical freshwater lake. Limnol. Oceanogr. 52, 1018–1025.

Hillmer, I., Imberger, J., 2007a. Influence of advection on scales of ecological studies in a coastal equilibrium flow. Continental Shelf Res. 27, 134–153.

Hillmer, I., Imberger, J., 2007b. Estimating in situ phytoplankton growth rates with a langrangian sampling strategy. Limnol. Oceanogr. Methods 5, 495–509.

Hodges, B., Imberger, J., Saggio, A., Winters, K., 2000. Modeling basin-scale internal waves in a stratified lake. Limnol. Oceanogr. 45, 1603–1620.

Hutchinson, G., 1961. The paradox of the plankton. Am. Nat. 95, 137–145.

Huisman, J., van Oostveen, P., Weissing, F.J., 1999. Critical depth and critical turbulence: two different mechanism for the development of phytoplankton blooms. Limnol. Oceanogr. 44, 1781–1787.

Imberger, J., Patterson, J., 1990. Physical limnology. Adv. Appl. Mech. 27, 303–475.

Jørgensen, S.E. (Ed.), 1994. Fundalmentals of Ecological Modeling, 2nd ed. Elsevier, Ámsterdam, p. 632.

Kierstead, H., Slobodkin, L., 1953. The size of water masses containing plankton blooms. J. Mar. Res. 12, 141–147.

Kromkamp, J., Walsby, A., 1990. A computer model of buoyancy and vertical migration in cyanobacteria. J. Plankton Res. 12, 161–183.

Laval, B., Hodges, B.R., Imberger, J., 2003. Reducing numerical diffusion effects with pycnocline filter. J. Hydraulic Eng. 129, 215–224.

Mero, F., 1978. Hydrology. In: Serruya, C. (Ed.), Lake Kinneret, Monogr. Biol., v. 32. W. Junk, The Hague, Netherlands, pp. 87–102.

Murray, A., 2001. The use of simple models in the design and calibration of a dynamic 2D model of a semi-enclosed Australian bay. Ecol. Modell. 136, 15–30.

Okubo, A., 1971. Oceanic diffusion diagrams. Deep-Sea Res. 18, 789–802.

Pollingher, U., Berman, T., 1975. Temporal and spatial patterns of dinoflagellate blooms in Lake Kinneret. Israel (1969–1974). Verh. Int. Verein. Limnol. 19, 1370–1382.

Pollingher, U., Zernel, E., 1981. *In situ* and experimental evidence of the influence of turbulence on cell division processes of *Peridinium cinctum fa*. Westii. (Lemm.). Lefevre. Br. Phycol. J. 16, 281–287.

Ptacnik, R., Diel, S., Berger, S., 2003. Performance of sinking and nonsinking phyotplankton taxa in a gradient of mixing depths. Limnol. Oceanogr. 48, 1903–1912.

Serruya, S., 1974. The mixing patterns of the Jordan River in Lake Kinneret. Limnol. Oceanogr. 19, 175–181.

Serruya, S., 1975. Wind, water temperature and motions in Lake Kinneret: general pattern. Verh. Int. Verein. Limnol. 19, 73–87.

Steele, J.H., Henderson, E.W., 1992. A simple model for plankton pathchiness. J. Plankton Res. 14, 1397–1403.

Stocker, R., Imberger, J., 2003. Horizontal transport and dispersion in the surface layer of a medium-sized lake. Limnol. Oceanogr. 48, 971–982.

Thomas, W.H., Gibson, C.H., 1990. Quantified small-scale turbulence inhibits a red tide dinoflagellate, *Gonyaulax polyedra* Stein. Deep-Sea Res. 37, 1583–1593.

Vilar, J.M.G., Solé, R.V., Rubí, J.M., 2003. On the origin of plankton patchiness. Physica A 317, 239–246.

Yeates, P.S., Imberger, J., 2004. Pseudo two-dimensional simulations of internal and boundary fluxes in stratified lakes and reservoirs. Int. J. River Basin Manage. 4, 1–23.

Zohary, T., 2004a. Changes to the phytoplankton assemblage of Lake Kinneret after decades of a predictable, repetitive pattern. Freshwater Biol. 49, 1355–1371.

Zohary, T. (Ed.), 2004b. Lake Kinneret Water Quality Management and Optimization Support System—Phase 2: Physiological Experiments. 6th Progress Report to the Israel Water Commission.

Zohary, T., Gal, G., Antenucci, J. (Eds.), 2006. Lake Kinneret Water Quality Management and Optimization Support System—Phase 2, Final Report to the Water Commission. IOLR-KLL report T1/2006.